

# Rational Design and Synthesis of an Orally Active Indolopyridone as a Novel Conformationally Constrained Cannabinoid Ligand Possessing Antiinflammatory Properties

Stephen T. Wrobleski,<sup>\*,†</sup> Ping Chen,<sup>†</sup> John Hynes, Jr.,<sup>†</sup> Shuqun Lin,<sup>†</sup> Derek J. Norris,<sup>†</sup> Chennagiri R. Pandit,<sup>†</sup> Steven Spergel,<sup>†</sup> Hong Wu,<sup>†</sup> John S. Tokarski,<sup>‡</sup> Xiaorong Chen,<sup>§</sup> Kathleen M. Gillooly,<sup>§</sup> Peter A. Kiener,<sup>§</sup> Kim W. McIntyre,<sup>§</sup> Vina Patil-koota,<sup>§</sup> David J. Shuster,<sup>§</sup> Lori A. Turk,<sup>§</sup> Guichen Yang,<sup>§</sup> and Katerina Leftheris<sup>†</sup>

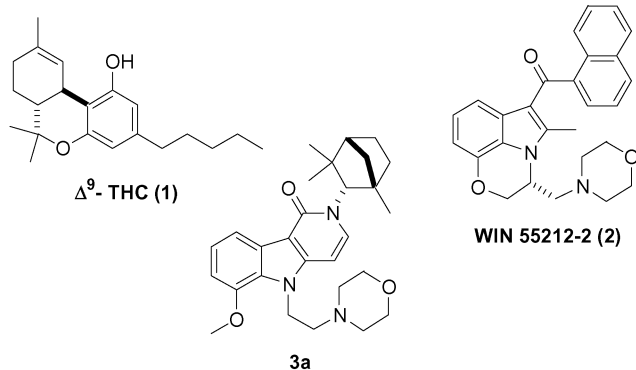
Departments of Discovery Chemistry, Structural Biology and Modeling, and Immunology, Inflammation, and Pulmonary Discovery, Bristol-Myers Squibb, P.O. Box 4000, Princeton, New Jersey 08543-4000

Received July 26, 2002

A series of unique indazoles and pyridoindolones have been rationally designed and synthesized as novel classes of cannabinoid ligands based on a proposed bioactive amide conformation. This has led to the discovery of the novel indolopyridone **3a** as a conformationally constrained cannabinoid ligand that displays high affinity for the CB2 receptor ( $K_i(\text{CB2}) = 1.0 \text{ nM}$ ) and possesses antiinflammatory properties when administered orally in an in vivo murine inflammation model.

## Introduction

The most widely known cannabinoid,  $\Delta^9$ -tetrahydrocannabinol ( $\Delta^9$ -THC, **1**), is considered to be the primary



psychoactive constituent of marijuana and is known to produce a variety of potentially beneficial therapeutic effects including analgesia, antiemesis, anticonvulsive, immunomodulation, and lowered intraocular pressure.<sup>1</sup> Unfortunately, the medical use of THC has been limited, as well as controversial, because of its often undesirable central nervous system (CNS) effects and potentially addictive properties. In an effort to identify the receptors responsible for cannabinoid activity, two cannabinoid receptor subtypes, CB1 and CB2 belonging to the GPCR superfamily of 7-transmembrane receptors, were first cloned in 1990 and 1993, respectively.<sup>2,3</sup> Early studies found the CB1 receptors to be highly expressed in the tissues of the central nervous system, while the CB2 receptors were detected mainly in peripheral tissues, particularly on the surface of immune cells.<sup>4</sup> As a result, it was widely believed that the CNS effects

of THC, as well as other cannabinoids, were predominantly mediated through the CB1 receptor whereas the immunomodulatory or antiinflammatory effects were mediated through the peripheral CB2 receptor subtype. More recent studies have suggested a broader tissue distribution of CB1 receptors,<sup>5</sup> and several reports have provided evidence for antiinflammatory effects mediated through the CB1 as well as CB2 receptors.<sup>6</sup>

In an effort to understand the role of cannabinoids and their receptors in biological responses, a significant amount of research effort has been focused on the identification of THC analogues as well as nonclassical or synthetic cannabinoids.<sup>7</sup> One of the most widely studied examples of the nonclassical type of cannabinoids is WIN-55212 (**2**), which belongs to the aminoalkylindole (AAI) class of compounds originally reported by Sterling-Winthrop in 1992.<sup>8</sup> This compound has been extensively investigated because of its high affinity toward the cannabinoid receptors ( $K_i(\text{CB1}) = 1.9 \text{ nM}$ ;  $K_i(\text{CB2}) = 0.3 \text{ nM}$ )<sup>9</sup> and has played an important role in the identification and characterization of the cannabinoid receptors and their associated functions. In addition, **2** is more active than the classical cannabinoid THC in several pharmacological and behavioral assays<sup>10</sup> and acts as an agonist toward cannabinoid receptors, resulting in a significant reduction of lipopolysaccharide (LPS) induced proinflammatory cytokine production (TNF- $\alpha$  and IL-1) in mice.<sup>6b,c</sup> Furthermore, a recent report has demonstrated the ability of **2** to inhibit LPS-induced TNF- $\alpha$  production in human peripheral blood monocytes (PBMCs).<sup>6a</sup>

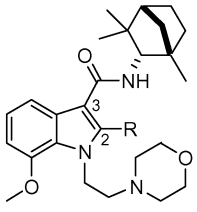
As part of our efforts to identify novel CB2 agonists as antiinflammatory agents, we have recently identified substituted indazoles and conformationally constrained indolopyridones as novel classes of cannabinoid ligands. This report describes the rational design and synthesis of these compounds leading to the identification of the novel indolopyridone **3a** as a potent cannabinoid ligand. In addition, the in vivo evaluation of **3a** as an antiin-

\* To whom correspondence should be addressed. Phone: 609-252-4873. Fax: 609-252-6601. E-mail: stephen.wrobleski@bms.com.

<sup>†</sup> Department of Discovery Chemistry.

<sup>‡</sup> Department of Structural Biology and Modeling.

<sup>§</sup> Department of Immunology, Inflammation, and Pulmonary Discovery.

**Table 1.** Effect of Indole C2 Substitution on Binding Affinity


compd	R	$K_i$ (nM)	
		CB2	CB1
<b>4a</b>	H	11 ± 3	245 ± 52
<b>4b</b>	methyl	29 ± 6	8 ± 2
<b>4c</b>	ethyl	110 ± 23	nd <sup>b</sup>
<b>4d</b>	<i>n</i> -propyl	6% <sup>a</sup>	nd <sup>b</sup>

<sup>a</sup> % inhibition at 100 nM ligand concentration. <sup>b</sup> Not determined.

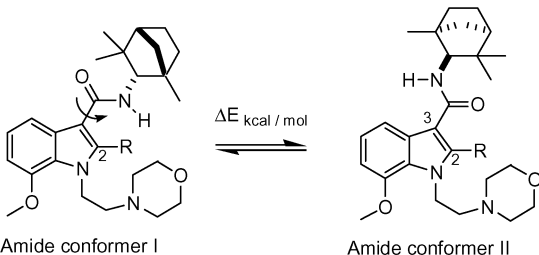
inflammatory agent using a murine model of inflammation is reported.

### Design

Previously, we have reported substituted indole C3 carboxamides bearing a (1*S*)-*endo*-fenchyl group as potent cannabinoid ligands.<sup>11</sup> Interestingly, analysis of the effects of C2 substitution on CB1 and CB2 binding affinity in this series revealed a strong preference for a small substituent at the C2 position as illustrated in Table 1. Only a hydrogen or methyl substituent was tolerated in obtaining good CB2 affinity as observed for compounds **4a** and **4b**. Increasing the size of the C2 substituent to ethyl as in **4c** or to *n*-propyl as in **4d** resulted in a significant decrease of CB2 binding affinity. Importantly, a similar trend of increasing size of the indole C2 substituent leading to decreased CB binding affinity has also been reported in the SAR analysis of **2** as well as other aminoalkylindole cannabinoid ligands.<sup>8,11</sup>

Despite having potent CB2 binding affinities, compounds **4a** and **4b** displayed only modest CB2 agonist activity as measured by the in vitro efficacy in inhibition of TNF- $\alpha$  release in human peripheral blood mononuclear cells (IC<sub>50</sub> = 13 and 33  $\mu$ M, respectively) relative to **2** in this assay (IC<sub>50</sub> = 6  $\mu$ M). In addition, the most potent compound **4a**, when administered orally up to a dose of 50 mg/kg, failed to show efficacy in a murine model of acute inflammation where LPS-induced TNF- $\alpha$  production was measured.<sup>11</sup> In light of these results, alternative chemotypes relative to the indole nucleus were pursued in an effort to identify, in vivo, orally active CB2 ligands.

The observed trend of a decrease in CB binding affinity in the indole series with an increase in the size of the C2 substituent was taken into consideration in the design of other potential chemotypes. It was rationalized that larger C2 substituents in the indole series may lead to decreased binding affinity by directly creating unfavorable contacts with receptor and/or indirectly by influencing the adjacent C3 amide rotamer population and position of the pendent fenchyl group. To investigate the influence of the C2 substituent on the C3 amide rotamer population, molecular modeling calculations in the form of torsional energy scans about the C3-carboxamide bond were performed on analogues **4a–d**. These calculations suggest two local minimum

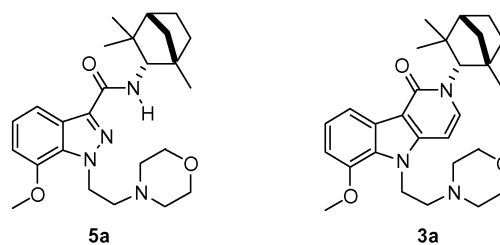
**Table 2.** Calculated Effect of C2 Substitution on Amide Conformations


compd	R	$\Delta E^a$ (kcal/mol)
<b>4a</b>	H	+0.6
<b>4b</b>	methyl	+2.9
<b>4c</b>	ethyl	+3.5
<b>4d</b>	<i>n</i> -propyl	+3.8

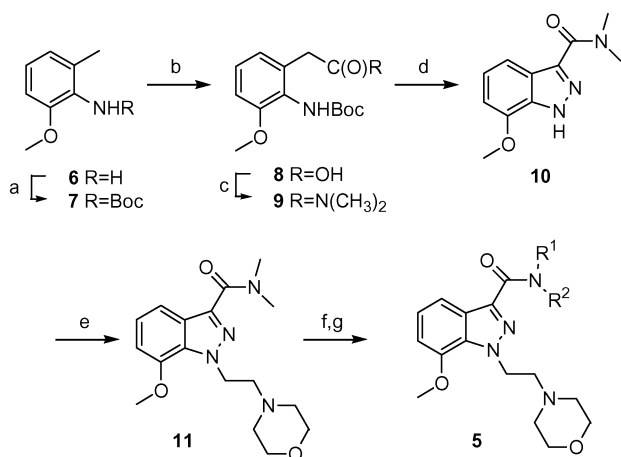
<sup>a</sup> (Energy of amide conformer I) – (energy of amide conformer II).

energy conformations about the C3-carboxamide bond depicted as amide conformer I and amide conformer II in Table 2. Both conformers maintain the amide group near the plane and in conjugation with the indole ring system. Furthermore, the DFT energy calculations suggest that the rotamer populations of the C3 amide group are most likely influenced by the size of the C2 group as illustrated in Table 2. More specifically, the calculated energy difference ( $\Delta E$ ) between conformers I and II indicate that conformer II is favored over conformer I in the range 0.6–3.8 kcal/mol for analogues **4a–d**. We rationalized that larger C2 substituents would destabilize conformer I relative to II because of unfavorable interactions between the C2 substituent and the amide nitrogen substituents. Interestingly, comparison of the CB2 binding affinities of **4a–d** listed in Table 1 with their respective amide conformational preferences as calculated in Table 2 suggests a trend of decreasing CB2 binding affinity with an increasing tendency to favor amide conformer II over conformer I. These results suggested to us that compounds that more strongly favor the amide conformer I may provide increased CB2 binding affinity. To further test this hypothesis, and in an attempt to identify compounds with increased cell potency relative to the indole analogues, chemotypes that would be expected to favor or adopt this amide orientation were pursued.

On the basis of DFT energy calculations performed identically to the calculations on the indole series, the proposed indazole **5a** was predicted to strongly favor



amide conformer I over conformer II by >4 kcal/mol. We rationalize that favorable stereoelectronic interactions between the indazole N-2 nitrogen and the amide hydrogen should stabilize conformer I relative to II. In addition, unfavorable stereoelectronic interactions between the N-2 nitrogen and the C3 carbonyl oxygen

Scheme 1<sup>a</sup>

<sup>a</sup> Conditions: (a) Boc anhydride, THF, reflux, 80%; (b) *n*BuLi, THF, -40 to -10 °C and then CO<sub>2</sub>, 80%; (c) EDCI, HOBt, Me<sub>2</sub>NH, DMF, room temp, 78%; (d) NaNO<sub>2</sub>, aqueous AcOH, 82%; (e) NaH, 4-(2-chloroethyl)morpholine hydrochloride, DMF, 45 °C, 72%; (f) aqueous NaOH, EtOH, 80 °C, 80%; (g) R<sup>1</sup>R<sup>2</sup>NH, EDCI, HOBt, (*i*Pr)<sub>2</sub>NEt, DMF, room temp, 66–87%.

would be expected to destabilize the alternative conformer **II** in the indazole case. In addition to **5a**, the novel indolopyridone **3a** was designed as a constrained analogue that would restrict the carboxamide to the desired orientation present in conformer **I**.

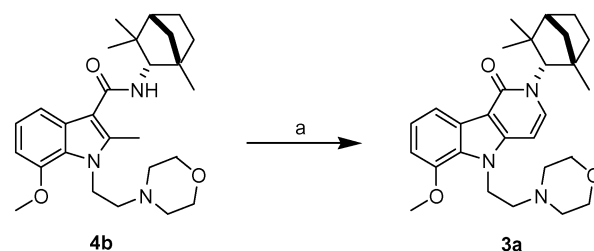
## Chemistry

Since the 7-methoxy substituent and the morpholinoethyl groups were previously found to be the optimal substitutions in the indole carboxamide series, the chemistry was initially designed to maintain these pharmacophores in the preparation of the indazole and indolopyridone chemotypes. Appropriately substituted indazoles were prepared from commercially available 2-methoxy-6-methylaniline (**6**) as outlined in Scheme 1. Protection of the aniline to afford **7**<sup>14</sup> followed by carboxylation and amide bond formation provided dimethylamide **9**. Sodium nitrite mediated cyclization<sup>15</sup> of **9** afforded indazole **10** that underwent a selective N-1 alkylation employing sodium hydride and commercially available 4-(2-chloroethyl)morpholine to provide **11**. Hydrolysis of the dimethylamide followed by amide bond formation with a variety of primary and secondary amines afforded the desired indazole products **5**.

The conformationally constrained indolopyridone analogues were easily synthesized from the previously prepared<sup>11</sup> 2-methyl-3-carboxamide indoles employing an efficient formylation and cyclization sequence<sup>16</sup> as illustrated by the synthesis of derivative **3a** in Scheme 2.

## Results and Discussion

All compounds were initially screened for CB2 binding affinity by displacement of radiolabeled **2**. Compounds at 100 nM concentration that gave >60% inhibition of **2** in binding to the CB2 receptor were subsequently screened for in vitro inhibition of TNF- $\alpha$  release in human peripheral blood mononuclear cells (PBMCs). Compounds that were active in the PBMC assay were then evaluated for oral activity in a murine model of acute inflammation where LPS-induced TNF- $\alpha$  produc-

Scheme 2<sup>a</sup>

<sup>a</sup> Conditions: (a) (1) 2.2 equiv of *n*BuLi, THF, -30 to 0 °C and then DMF, (2) 3 N aqueous HCl, 55 °C, 85%.

Table 3. Selected Indazole Carboxamides **5a–d**

R	K <sub>i</sub> (CB2) (nM)	TNF- $\alpha$ (PBMC) IC <sub>50</sub> ( $\mu$ M) <sup>b</sup>	K <sub>i</sub> (CB1) (nM)
<b>5a</b> HN[(1 <i>S</i> )-fenchyl]	2.0 $\pm$ 0.5	30	24 $\pm$ 10
<b>5b</b> HN[ $\alpha$ -(2-pyridyl)benzyl] <sup>a</sup>	146 $\pm$ 79	20	162 $\pm$ 60
<b>5c</b> HN[(2)-methoxybenzyl]	77 $\pm$ 20	43	nd <sup>c</sup>
<b>5d</b> N[(N-2-propyl)(2-chloro-6-fluorobenzyl)]	69 $\pm$ 26	36	nd <sup>c</sup>

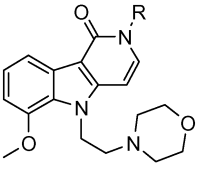
<sup>a</sup> Racemic. <sup>b</sup> *n* = 1. <sup>c</sup> Not determined.

tion was measured. For selected compounds, CB1 receptor affinities were also determined by displacement of radiolabeled **2** from the CB1 receptor.

**Indazole Series.** By use of the previously outlined synthesis, four indazoles **5a–d** were identified as having appreciable CB2 binding affinity (IC<sub>50</sub> < 200 nM). Analogous to the indole series, the (1*S*)-fenchylamide analogue **5a** provided the highest CB2 and CB1 binding affinity within the indazole series (K<sub>i</sub>(CB2) = 2.0  $\pm$  0.5 nM; K<sub>i</sub>(CB1) = 24  $\pm$  10 nM). In addition, indazole **5a** showed an increase in CB2 binding affinity relative to the most potent indole fenchylamide **4a** (K<sub>i</sub>(CB2) = 11  $\pm$  3 nM; K<sub>i</sub>(CB1) = 245  $\pm$  52 nM) in the CB2 and CB1 assays. These initial results appeared to support our hypothesis that compounds that favor the amide conformer **I** based on molecular modeling may provide increased affinity for the CB2 receptor (vide supra). Unfortunately, despite having excellent CB2 and CB1 binding affinity, indazoles **5a–d** showed minimal agonist activity at the CB2 receptor, resulting in only moderate cell potency against TNF- $\alpha$  production in the PBMC cell assay (IC<sub>50</sub> = 20–43  $\mu$ M) as listed in Table 3. In light of these results, the indazole analogues were abandoned from further in vivo studies and attention was focused on evaluating the conformationally constrained indolopyridone derivatives.

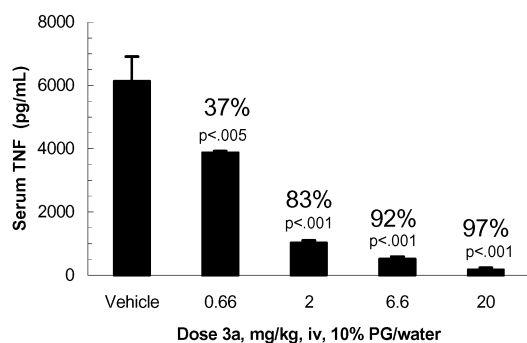
**Indolopyridone Series.** Three out of four of the amide analogues that were prepared in the indazole series were synthesized and evaluated in the corresponding indolopyridone series as listed in Table 4. As in the previous indole and indazole cases, the (1*S*)-fenchyl analogue **3a** was the most potent CB2 ligand in the indolopyridone series (K<sub>i</sub>(CB2) = 1.0  $\pm$  0.2 nM). In addition, indolopyridone **3a** was the most potent CB2 ligand compared to any of the indole or indazole derivatives prepared to date. Interestingly, indolopyridone **3b**



**Table 4.** Selected Substituted Indolopyridones **3a–c**


R	$K_i$ (CB2) (nM)	TNF- $\alpha$ (PBMC) IC <sub>50</sub> ( $\mu$ M)	$K_i$ (CB1) (nM)
<b>3a</b> (1 <i>S</i> )-fenchyl	1.0 $\pm$ 0.2	8 $\pm$ 4 <sup>b</sup>	16 $\pm$ 4
<b>3b</b> (2)-methoxybenzyl	67 $\pm$ 23	7 $\pm$ 7 <sup>b</sup>	3700 $\pm$ 1000
<b>3c</b> $\alpha$ -(2-pyridyl)benzyl <sup>a</sup>	13% <sup>c</sup>	nd <sup>d</sup>	nd <sup>d</sup>

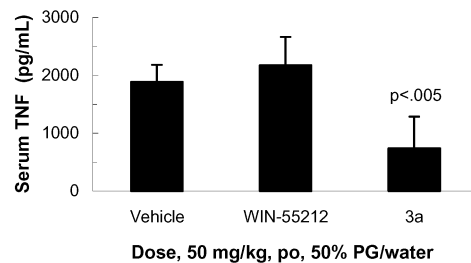
<sup>a</sup> Racemic. <sup>b</sup>  $n = 4$ . <sup>c</sup> % inhibition at 500  $\mu$ M. <sup>d</sup> Not determined.

**Figure 1.** The iv dose–response of **3a** in LPS-induced TNF- $\alpha$  release in mice ( $n = 8$  animals/group).

( $K_i$ (CB2) = 67  $\pm$  23 nM) containing the 2-methoxybenzylamide was similar in potency toward the CB2 receptor compared to its indazole counterpart **5c** ( $K_i$ (CB2) = 77  $\pm$  20 nM). In contrast, the indolopyridone **3c** containing the  $\alpha$ -(2-pyridyl)benzyl substituent appeared less active at the CB2 receptor (13% inhibition at 500  $\mu$ M) compared to indazole **5b** ( $K_i$ (CB2) = 146  $\pm$  79 nM). Most gratifyingly, however, indolopyridone **3a** showed increased cell activity (IC<sub>50</sub> = 8  $\mu$ M) relative to the most potent indole and indazoles **4a** and **5a** (IC<sub>50</sub> = 13 and 30  $\mu$ M, respectively). In addition, the 2-methoxybenzylamide **3b** also gave an increase in cell activity (IC<sub>50</sub> = 7  $\mu$ M) relative to its indazole counterpart **5c** (IC<sub>50</sub> = 43  $\mu$ M) despite having similar CB2 binding affinities. After identification of indolopyridone **3a** as the most potent CB2 ligand with significant cell activity, **3a** was evaluated in an in vivo model.

Indolopyridone **3a** exhibited a dose-dependent inhibition of LPS-stimulated TNF- $\alpha$  release when dosed intravenously, having an ED<sub>50</sub> between 0.66 and 2 mg/kg as illustrated in Figure 1. In addition, **3a** was also orally efficacious resulting in a 61% reduction of serum TNF- $\alpha$  levels when dosed at 50 mg/kg as shown in Figure 2. It is noteworthy to mention that **2** did not show any efficacy in this murine inflammation model when administered orally.

In conclusion, molecular modeling calculations and conformation–activity relationships within a class of indole-derived cannabinoid ligands have suggested the involvement of the amide conformer **I** as a bioactive conformation at the CB2 receptor. This hypothesis has been used to rationally design novel, conformationally restricted indazole and indolopyridone ligands having an increased affinity for the CB2 receptor. Most impor-

**Figure 2.** In vivo activity of CB ligands dosed orally in inhibiting LPS-induced TNF- $\alpha$  release in mice ( $n = 8$  animals/group).

tantly, this work had led to the identification of indolopyridone **3a** as a potent and orally active cannabinoid ligand that possesses antiinflammatory properties in vivo when administered in a murine inflammation model.

## Experimental Section

**Chemistry.** Proton magnetic resonance (<sup>1</sup>H NMR) spectra were recorded on a Bruker ARX-400 spectrometer and are reported in ppm relative to the reference solvent of the sample in which they were run. HPLC and LC–MS analyses were conducted using a Shimadzu LC-10AS liquid chromatograph and a SPD UV–vis detector at 220 nm with the MS detection performed with a Micromass Platform LC spectrometer. HPLC analyses were performed using the following conditions: Ballistic YMC S5 ODS 4.6 mm  $\times$  50 mm column with a binary solvent system where solvent A is 10% methanol, 90% water, and 0.2% phosphoric acid and solvent B is 90% methanol, 10% water, and 0.2% phosphoric acid; flow rate = 4 mL/min; linear gradient time = 4 min; start %B = 0, final %B = 100. LC–MS analyses were performed using the following conditions: Waters Xterra 5  $\mu$ m, 4.6 mm  $\times$  30 mm column with a binary solvent system where solvent A is 10% methanol, 90% water, and 0.1% trifluoroacetic acid and solvent B is 90% methanol, 10% water, and 0.1% trifluoroacetic acid; flow rate = 4 mL/min; linear gradient time = 2 min; start %B = 0, final %B = 100. Melting points were measured on a Mel-Temp 3.0 melting point apparatus and are uncorrected. All reagents were purchased from commercial sources unless otherwise noted. Preparation of (1*S*)-endo-fenchylamine was performed according to the previously reported procedures.<sup>17</sup> All reagents were used without further purification unless otherwise noted. All reactions were performed under an argon atmosphere. Reactions in aqueous media were run under an ambient atmosphere unless otherwise noted.

**[3-Methoxy-2-(*tert*-butyloxycarbonylamino)]phenylacetic Acid (**8**).** To 73 mL (73 mmol) of a 1 M solution of di-*tert*-butyl dicarbonate in THF at room temperature was added 10 g (73 mmol) of 3-methoxy-2-(*tert*-butyloxycarbonylamino)-toluene, and the resulting solution was refluxed for 24 h. The mixture was cooled to room temperature and concentrated on a rotary evaporator. The resulting viscous oil was dissolved in methylene chloride (125 mL), and the solution was successively washed with 6% aqueous citric acid (2  $\times$  30 mL), water (2  $\times$  30 mL), and brine (30 mL) and then dried over anhydrous sodium sulfate, filtered, and concentrated in vacuo to afford the crude product as a viscous oil. The resulting oil was dissolved in a minimal amount of warm methylene chloride (~30 mL), and hexanes were added (~125 mL). The cloudy mixture was cooled to 0  $^{\circ}$ C for 1 h. The crystalline product was collected by filtration and dried in vacuo to afford 13.9 g (80%) of **8** as a white solid: mp 161.3–162.4  $^{\circ}$ C. <sup>1</sup>H NMR (400 MHz, MeOH-*d*<sub>4</sub>):  $\delta$  7.19 (t,  $J = 8.2$  Hz, 1H), 6.93 (d,  $J = 8.3$  Hz, 1H), 6.89 (d,  $J = 7.7$  Hz, 1H), 3.82 (s, 3H), 3.61 (s, 2H), 1.48 (br s, 9H). HPLC:  $t_R = 2.41$  min, 99.2% purity. HRMS (EI)  $m/z$  calcd for C<sub>14</sub>H<sub>18</sub>NO<sub>5</sub> [M – H]<sup>+</sup>: 280.1185. Found: 280.1174.

**[3-Methoxy-2-(*tert*-butyloxycarbonylamino)]phenylacetic Acid Dimethylacetamide (**9**).** To a solution of 8.32 g

(29.6 mmol) of **8**, 8.51 g (44.4 mmol) of 1-(3-dimethylamino-propyl)-3-ethylcarbodiimide hydrochloride, 4.80 g (35.5 mmol) of 1-hydroxybenzotriazole, and 9.66 g (118 mmol) of dimethylamine hydrochloride in 90 mL of dimethylformamide at room temperature was added 25.8 mL (148 mmol) of diisopropylethylamine, and the resulting solution was stirred for 48 h. The reaction mixture was concentrated in vacuo, and the resulting oil was dissolved in 350 mL of dichloromethane and washed with aqueous 1 N sodium hydroxide (3 × 125 mL), 6% aqueous citric acid solution (3 × 100 mL), water (100 mL), and brine (100 mL). After the mixture was dried over anhydrous sodium sulfate, the resulting solution was decanted and concentrated on a rotary evaporator to afford a reddish-orange oil as the crude product. This material was dissolved in diethyl ether (ca. 100 mL) and re-concentrated on the rotary evaporator, yielding a yellow solid that was subsequently triturated with two 35-mL portions of hexanes to remove any residual dimethylformamide. The resulting solid was dried in vacuo to deliver 7.09 g (78%) of **9** as a yellow solid: mp 111.8–113.0 °C. <sup>1</sup>H NMR (400 MHz, MeOH-*d*<sub>4</sub>): δ 7.20 (t, *J* = 8.0 Hz, 1H), 6.93 (d, *J* = 8.4 Hz, 1H), 6.79 (d, *J* = 7.7 Hz, 1H), 3.82 (s, 3H), 3.71 (s, 2H), 2.99 (s, 3H), 2.95 (s, 3H), 1.47 (br s, 9H). HPLC: *t*<sub>R</sub> = 2.46 min, 99.0% purity. HRMS (EI) *m/z* calcd for C<sub>16</sub>H<sub>25</sub>N<sub>2</sub>O<sub>4</sub> [M + H]<sup>+</sup>: 309.1814. Found: 309.1812.

**7-Methoxy-3-dimethylamidoindazole (10)**. To a stirring solution of 1.27 g (4.12 mmol) of **9** in 4% aqueous acetic acid at 95 °C was slowly added an aqueous solution of 0.85 g (12.4 mmol) of sodium nitrite in 1.4 mL of water over 2 h. After the addition was complete, HPLC analysis showed nearly complete consumption of the substrate. The reaction mixture was cooled to room temperature and concentrated on a rotary evaporator, and the resulting solid was suspended in approximately 30 mL of water. The product was collected by vacuum filtration, washed with water (20 mL), and then dried in vacuo to afford 0.74 g (82%) of **10** as a yellow solid: mp 224.5–226.2 °C. <sup>1</sup>H NMR (400 MHz, MeOH-*d*<sub>4</sub>): δ 7.47 (t, *J* = 8.5 Hz, 1H), 7.13 (t, *J* = 7.8 Hz, 1H), 6.85 (d, *J* = 7.6 Hz, 1H), 4.01 (s, 3H), 3.36 (s, 3H), 3.18 (s, 3H). HPLC: *t*<sub>R</sub> = 2.10 min, 99.1% purity. HRMS (EI) *m/z* calcd for C<sub>11</sub>H<sub>14</sub>N<sub>3</sub>O<sub>2</sub> [M + H]<sup>+</sup>: 220.1086. Found: 220.1080.

**7-Methoxy-*N,N*-dimethyl-1-[2-(4-morpholinyl)ethyl]-1*H*-indazole-3-carboxamide (11)**. To a room-temperature solution of 0.549 g (2.50 mmol) of **10** and 0.75 g (5.00 mmol) of 4-(2-chloroethyl)morpholine in 5 mL of anhydrous dimethylformamide was added 0.20 g (5.0 mmol) of 60% sodium hydride dispersion in two portions over 10 min. The reaction mixture was stirred for 14 h, and then an additional 0.75 g (5.0 mmol) of 4-(2-chloroethyl)morpholine was added followed by heating to 40 °C for an additional 2 h. The reaction mixture was cooled to room temperature, and 10 mL of water was slowly added. The mixture was extracted with ethyl acetate (4 × 30 mL), and the combined extracts were washed with water (3 × 7 mL) and brine (7 mL), then dried over anhydrous sodium sulfate, decanted, and concentrated in vacuo to afford a yellow liquid that partially solidified upon standing. This material was triturated with three 20-mL portions of hexanes and the remaining white solid was dried in vacuo to afford 0.60 g (72%) of **11**: mp 109.5–110.3 °C. <sup>1</sup>H NMR (400 MHz, MeOH-*d*<sub>4</sub>): δ 7.49 (d, *J* = 8.2 Hz, 1H), 7.14 (t, *J* = 7.8 Hz, 1H), 6.89 (d, *J* = 7.6 Hz, 1H), 4.82 (t, *J* = 6.7 Hz, 2H), 4.00 (s, 3H), 3.62–3.60 (m, 4H), 3.37 (s, 3H), 3.17 (s, 3H), 2.87 (t, *J* = 6.7 Hz, 2H), 2.53–2.51 (m, 4H). HPLC: *t*<sub>R</sub> = 1.46 min, 99.4% purity. HRMS (EI) *m/z* calcd for C<sub>17</sub>H<sub>25</sub>N<sub>4</sub>O<sub>3</sub> [M + H]<sup>+</sup>: 333.1927. Found: 333.1914.

**7-Methoxy-1-[2-(4-morpholinyl)ethyl]-*N*-[(1*S*,2*S*)-1,3,3-trimethylbicyclo[2.2.1]heptan-2-yl]-1*H*-indazol-3-carboxamide (5a)**. To 100 mg (0.30 mmol) of **11** was added 0.5 mL of 3 N aqueous sodium hydroxide and 0.5 mL of ethanol, and the resulting solution was heated at 80 °C for 16 h and then cooled to room temperature and concentrated. The residue was dissolved in water (5 mL) and adjusted to pH 7 by addition of 1 N aqueous HCl and then was re-concentrated. The resulting residue was redissolved in water (5 mL) and made basic (greater than pH 10) by adding a few drops of 1 N aqueous

sodium hydroxide. The aqueous solution was concentrated on a rotary evaporator, and the remaining solid was azeotroped with toluene, dissolved in methylene chloride (ca. 10 mL), dried over anhydrous sodium sulfate, filtered, and concentrated in vacuo to afford 79 mg (80%) of a white solid as the sodium carboxylate salt. This compound was used directly in the next step without further purification.

To the sodium carboxylate salt (79 mg, 0.23 mmol) were successively added 65 mg (0.34 mmol) of EDCl, 38 mg (0.28 mmol) of HOBt, 0.6 mL of DMF, 0.16 mL (0.92 mmol) of diisopropylethylamine, and 53 mg (28 mmol) of (1*S*)-*endo*-fenchylamine.<sup>17</sup> The resulting mixture was stirred at 70 °C for 16 h and then cooled to ambient temperature, and 20 mL of ethyl acetate was added. The mixture was successively washed with saturated aqueous sodium bicarbonate (3 × 5 mL), water (2 × 5 mL), and brine (5 mL), and the organic solution was dried over anhydrous sodium sulfate, filtered, and concentrated in vacuo to afford the crude product. Purification by flash chromatography on silica gel using 5% methanol in ethyl acetate as the eluant afforded 91 mg (87%) of **5a** as a white solid. <sup>1</sup>H NMR (400 MHz, MeOH-*d*<sub>4</sub>): δ 7.79 (d, *J* = 8.2 Hz, 1H), 7.25 (t, *J* = 8.0 Hz, 1H), 7.00 (d, *J* = 7.6 Hz, 1H), 4.87–4.85 (m, 2H), 4.07 (s, 1H), 4.06 (overlapping s, 3H), 3.83–3.78 (m, 6H), 3.63 (br s, 2H), 3.30 (br s, 2H), 1.83–1.76 (m, 3H), 1.60–1.54 (m, 2H), 1.35–1.22 (m, 2H), 1.19 (s, 3H), 1.12 (s, 3H), 0.09 (s, 3H). HPLC: *t*<sub>R</sub> = 2.92 min, 98.9% purity. LC-MS: *t*<sub>R</sub> = 1.80 min, [M + H]<sup>+</sup> = 441.5. HRMS (EI) *m/z* calcd for C<sub>25</sub>H<sub>37</sub>N<sub>4</sub>O<sub>3</sub> [M + H]<sup>+</sup>: 441.2866. Found: 441.2885.

**7-Methoxy-*N*-[phenyl(2-pyridinyl)methyl]-1-[2-(4-morpholinyl)ethyl]-1*H*-indazole-3-carboxamide (5b)**. **5b** was prepared as described for **5a** to obtain 26 mg (66%) of **5b** as a yellow solid. <sup>1</sup>H NMR (400 MHz, MeOH-*d*<sub>4</sub>): δ 8.58 (dd, *J* = 4.3, 0.9 Hz, 1H), 7.79 (td, *J* = 7.7, 1.7 Hz, 1H), 7.72 (d, *J* = 8.3 Hz, 1H), 7.50 (d, *J* = 7.9 Hz, 1H), 7.41 (d, *J* = 8.6 Hz, 2H), 7.34–7.30 (m, 3H), 7.26–7.22 (m, 1H), 7.14 (t, *J* = 7.9 Hz, 1H), 6.87 (d, *J* = 7.6 Hz, 1H), 6.38 (s, 1H), 4.85 (t, *J* = 6.9 Hz, 2H), 3.99 (s, 3H), 3.62 (t, *J* = 4.6 Hz, 4H), 2.88 (t, *J* = 6.9 Hz, 2H), 2.54 (t, *J* = 4.4 Hz, 4H). HPLC: *t*<sub>R</sub> = 2.07 min, 99.0% purity. LC-MS: *t*<sub>R</sub> = 1.35 min, [M + H]<sup>+</sup> = 472.8. HRMS (EI) *m/z* calcd for C<sub>27</sub>H<sub>30</sub>N<sub>5</sub>O<sub>3</sub> [M + H]<sup>+</sup>: 472.2349. Found: 472.2343.

**7-Methoxy-*N*-[(2-methoxyphenyl)methyl]-1-[2-(4-morpholinyl)ethyl]-1*H*-indazole-3-carboxamide (5c)**. **5c** was prepared as described for **5a** to obtain 18 mg (77%) of **5c** as an off-white solid. <sup>1</sup>H NMR (400 MHz, MeOH-*d*<sub>4</sub>): δ 7.76 (d, *J* = 8.1 Hz, 1H), 7.29 (d, *J* = 7.4 Hz, 1H), 7.25 (td, *J* = 8.1, 1.5 Hz, 1H), 7.15 (t, *J* = 7.9 Hz, 1H), 6.97 (d, *J* = 8.1 Hz, 1H), 6.92–6.86 (m, 2H), 4.81 (t, *J* = 6.9 Hz, 2H), 4.60 (s, 2H), 3.99 (s, 3H), 3.89 (s, 3H), 3.61 (t, *J* = 4.7 Hz, 4H), 2.86 (t, *J* = 6.9 Hz, 2H), 2.51 (t, *J* = 4.4 Hz, 4H). HPLC: *t*<sub>R</sub> = 2.27 min, 98.4% purity. LC-MS: *t*<sub>R</sub> = 1.48 min, [M + H]<sup>+</sup> = 425.3. HRMS (EI) *m/z* calcd for C<sub>23</sub>H<sub>29</sub>N<sub>4</sub>O<sub>4</sub> [M + H]<sup>+</sup>: 425.2189. Found: 425.2203.

***N*-[(2-Chloro-6-fluorophenyl)methyl]-7-methoxy-*N*-[(1-methylethyl)-1-[2-(4-morpholinyl)ethyl]-1*H*-indazole-3-carboxamide (5d)**. **5d** was prepared as described for **5a** to obtain 21 mg (75%) of **5d** as a pale-yellow solid. <sup>1</sup>H NMR (400 MHz, MeOH-*d*<sub>4</sub>): δ 7.51–7.49 (m, 1H), 7.28–7.22 (m, 2H), 7.14 (d, *J* = 7.9 Hz, 1H), 7.12–7.03 (m, 1H), 6.89 (d, *J* = 7.6 Hz, 1H), 5.32 (br s, 2H), 4.79 (br s, 2H), 4.00 (s, 3H), 3.60–3.51 (m, 5H), 2.88–2.80 (m, 2H), 2.45 (br s, 4H), 1.25–1.13 (m, 6H). HPLC: *t*<sub>R</sub> = 2.79 min, 98.8% purity. LC-MS: *t*<sub>R</sub> = 1.74 min, [M + H]<sup>+</sup> = 489.3. HRMS (EI) *m/z* calcd for C<sub>25</sub>H<sub>31</sub>ClFN<sub>4</sub>O<sub>3</sub> [M + H]<sup>+</sup>: 489.2069. Found: 489.2071.

**2,5-Dihydro-6-methoxy-5-[2-(4-morpholinyl)ethyl]-2-[(1*S*,2*S*)-1,3,3-trimethylbicyclo[2.2.1]heptan-2-yl]-1*H*-pyrido[4,3-*b*]indol-1-one (3a)**. To a solution of **4b**<sup>11</sup> (0.20 g, 0.44 mmol) in 4 mL of anhydrous THF at –30 °C was added 0.88 mL (1.3 mmol) of a 1.5 M solution of *n*BuLi in hexanes, and the resulting solution was warmed to room temperature over 45 min. The solution was cooled to –30 °C, DMF (0.14 mL, 1.8 mmol) was added, and the mixture was stirred at –30 °C for 15 min and then at room temperature for 1 h. The reaction mixture was transferred via cannula into 6 mL of a well-stirred 10% aqueous HCl solution that had been deoxygenated by bubbling argon through the solution for approximately 10 min



prior to the addition. The mixture was heated to 55 °C for 17 h, cooled to room temperature, and made basic by a dropwise addition of 3 N aqueous KOH to a pH of approximately 10. The mixture was extracted with methylene chloride (3 × 20 mL), washed with water (20 mL) and brine (10 mL), dried over sodium sulfate, and concentrated in vacuo to afford the crude product as a yellow semisolid. The crude product was purified by flash chromatography on silica gel using a gradient elution of 80% ethyl acetate in hexanes initially and then 100% ethyl acetate to elute the product. Concentration of the desired fractions in vacuo provided 0.17 g (85%) of **3a** as an off-white solid: mp 164.4–165.4 °C. <sup>1</sup>H NMR (400 MHz, CDCl<sub>3</sub>): δ 8.09 (d, *J* = 7.8 Hz, 1H), 7.65 (d, *J* = 7.7 Hz, 1H), 7.22 (app t, *J* = 8.0 Hz, 1H), 6.86 (d, *J* = 8.0 Hz, 1H), 6.40 (d, *J* = 7.7 Hz, 1H), 5.29 (s, 1H), 4.62 (t, *J* = 6.9 Hz, 2H), 3.99 (s, 3H), 3.72–3.70 (m, 4H), 2.78 (t, *J* = 7.4 Hz, 2H), 2.57–2.54 (m, 4H), 2.06–1.96 (m, 3H), 1.78–1.60 (m, 1H), 1.39–1.34 (m, 3H), 1.34 (overlapping s, 3H), 1.09 (s, 3H), 0.95 (s, 3H). HPLC: *t*<sub>R</sub> = 2.80 min, 99.5% purity. LC–MS: *t*<sub>R</sub> = 1.77 min, [M + H]<sup>+</sup> = 464.5. HRMS (EI) *m/z* calcd for C<sub>28</sub>H<sub>38</sub>N<sub>3</sub>O<sub>3</sub> [M + H]<sup>+</sup>: 464.2913. Found: 464.2914. Anal. (C<sub>28</sub>H<sub>37</sub>N<sub>3</sub>O<sub>3</sub>) C, H, N.

**2,5-Dihydro-6-methoxy-2-(2-methoxyphenyl)-5-[2-(4-morpholinyl)ethyl]-1H-pyrido[4,3-*b*]indol-1-one (3b).** **3b** was prepared as described for **3a** to obtain 38 mg of **3b** as a yellow solid. <sup>1</sup>H NMR (400 MHz, CDCl<sub>3</sub>): δ 8.64 (d, *J* = 5.0 Hz, 1H), 8.05 (d, *J* = 8.0 Hz, 1H), 7.80 (s, 1H), 7.69 (t, *J* = 7.7 Hz, 1H), 7.54 (d, *J* = 7.6 Hz, 1H), 7.42 (d, *J* = 7.9 Hz, 1H), 7.36–7.30 (m, 3H), 7.28–7.18 (m, 4H), 6.83 (d, *J* = 7.9 Hz, 1H), 6.43 (d, *J* = 7.6 Hz, 1H), 4.59 (app t, *J* = 6.8 Hz, 2H), 3.96 (s, 3H), 3.70–3.67 (m, 4H), 2.73 (app t, *J* = 6.8 Hz, 2H), 2.53–2.50 (m, 4H). HPLC: *t*<sub>R</sub> = 1.91 min, 98.6% purity. LC–MS: *t*<sub>R</sub> = 1.93 min, [M + H]<sup>+</sup> = 495.1. HRMS (EI) *m/z* calcd for C<sub>30</sub>H<sub>31</sub>N<sub>4</sub>O<sub>3</sub> [M + H]<sup>+</sup>: 495.2396. Found: 495.2381.

**2,5-Dihydro-6-methoxy-5-[2-(4-morpholinyl)ethyl]-2-phenyl(2-pyridinyl)methyl]-1H-pyrido[4,3-*b*]indol-1-one (3c).** **3c** was prepared as described for **3a** to obtain 68 mg (55%) of **3c** as a light-orange solid. <sup>1</sup>H NMR (400 MHz, CDCl<sub>3</sub>): δ 8.08 (d, *J* = 7.9 Hz, 1H), 7.43 (d, *J* = 7.5 Hz, 1H), 7.31 (d, *J* = 7.9 Hz, 1H), 7.26–7.19 (m, 4H), 6.92–6.88 (m, 2H), 6.84 (d, *J* = 7.9 Hz, 1H), 6.42 (d, *J* = 7.5 Hz, 1H), 4.60 (app t, *J* = 7.0 Hz, 2H), 3.97 (s, 3H), 3.88 (s, 3H), 3.69 (app t, *J* = 4.4 Hz, 4H), 2.74 (t, *J* = 7.9 Hz, 2H), 2.53 (t, *J* = 4.4 Hz, 4H). HPLC: *t*<sub>R</sub> = 2.91 min, 98.1% purity. LC–MS: *t*<sub>R</sub> = 1.84 min, [M + H]<sup>+</sup> = 448.2. HRMS (EI) *m/z* calcd for C<sub>26</sub>H<sub>30</sub>N<sub>3</sub>O<sub>4</sub> [M + H]<sup>+</sup>: 448.2236. Found: 448.2236.

**Molecular Modeling.** The modeling was performed on an SGI Octane workstation. The starting coordinates of the structures were generated using CONCORD. The conformational profiles of the compounds were examined by a 5000-step Monte Carlo (MC) conformational search using Batchmin as implemented in Macromodel<sup>18</sup> (version 7.0) using the Merck molecular mechanics force field<sup>19</sup> (MMFF) and the GB/SA water continuum model. The trial conformation from each MC step was subjected to conjugate gradient minimization using the Polak–Ribiere first derivative method until a derivative convergence criterion of 0.01 kcal mol<sup>-1</sup> Å<sup>-1</sup> was reached or until a maximum of 400 iterations had been performed. The resulting unique conformations within a 20 kcal/mol energy window (a conformation was deemed unique if it met a heavy atom root-mean-square criterion of >0.25 Å compared to an existing conformer) were further subjected to 500 steps of conjugate gradient minimization. The pool of conformations of each compound, within an energy window of 10 kcal/mol, was reduced by means of cluster analysis (Xcluster<sup>20</sup> option implemented in Macromodel). The unique conformations were subjected to 30 steps of DFT energy optimizations as implemented in Jaguar<sup>21</sup> (version 4.0) at B3LYP/G-31G\*\*, and a single-point energy was calculated for the resulting geometries using B3LYP/cc-PVTZ-(f)<sup>+</sup>. The grid torsional energy scans about the C3–carboxamide bond were performed from 0° to 330° in 30° increments using the same energy optimization protocol as for the unique set of Monte Carlo conformations. The scans were performed on the core part of the molecules

with a methyl group on N1 instead of the morpholinoethyl group to increase the efficiency of calculations. Because the morpholinoethyl group can adopt similar conformations for all the analogues and does not affect the conformation about the C3–carboxamide bond, it was felt that this was a reasonable approximation. The conformation of the C2 substituent was that conformation found to give the lowest energy in the Monte Carlo simulations.

**CB2 and CB1 Assay Protocol.** The following assay has been carried out using the human cannabinoid receptor expressed in Chinese hamster ovary (CHO) cells. Radioactive tracer label (WIN 55,212-2 mesylate [5,7-<sup>3</sup>H] for CB2, CP55,940 for CB1) and test compounds are incubated together in a 96-well tissue culture plate. All reagents are dissolved or resuspended in binding buffer (10 mM HEPES, pH 7.4, 1 mM EDTA, 5 mM MgCl<sub>2</sub>, 0.3% BSA). The reaction is initiated by the addition of membranes (50 mg) from CHO-K1 cells expressing either CB1 or CB2. The plates are incubated 2 h with shaking at room temperature, and the reaction mixture is harvested on a Wallac Filtermat B with seven wash cycles using wash buffer (10 mM HEPES, pH 7.4, 0.1% BSA). The filter is counted in a Betaplate scintillation counter to ascertain the cannabinoid inhibitory activity of the test compound (activity inversely proportional to the amount of labeled WIN55,212-2 incorporated). Routinely the radiolabel was used at a concentration of 10 nM, but the exact concentration of reagents and the amount of label can be varied as needed.

**PBMC Assay Protocol.** Human PBMCs were isolated from whole blood collected from healthy donors. Blood was diluted into RPMI 1640 (Life Technologies) containing 2.5 mM EDTA (Life Technologies) and 10 μg/mL polymyxin (Sigma), and then it was underlaid with ficoll (Accurate Scientific Co.) and centrifuged at 600*g* for 25 min. The interface is collected, and cells are washed twice and resuspended in RPMI, 10% FBS. Cells are then distributed (200 μL/well) into 96-well tissue culture treated plates (Falcon) at 1 × 10<sup>6</sup> cells/mL in RPMI, 10% FBS. Test compounds were added to appropriate wells and incubated with cells for 30 min. Cells were then stimulated by the addition of lipopolysaccharide (LPS, BioWhittaker), with a final concentration of 25 ng/mL, and incubated for 6 h at 37 °C. The cell supernatants were removed and assayed for TNF-α by ELISA (R&D Systems).

**Inhibition of TNF-α Release in Mice.** BALB/c female mice, 6–8 weeks of age, were obtained from Harlan laboratories and maintained ad libitum on water and standard rodent chow (Harlan Teklad). Mice were acclimated to ambient conditions for at least 1 week prior to use. For intravenous (iv) dosing, the compounds were prepared in a solution of 10% propylene glycol in phosphate-buffered saline. Lipopolysaccharide (LPS, *E. coli* O111:B4; Sigma) was added to the dosing solution at a final concentration of 10 μg/mL. The mixture was injected in a total volume of 0.1 mL per mouse. Blood samples were obtained 60 min after the compound + LPS injection. For oral dosing, the compounds were prepared in a solution of 50% propylene glycol in water and a dosing volume of 0.2 mL per mouse was administered by gavage 10 min prior to LPS injection (0.1 mL of LPS suspended at 10 μg/mL in PBS, administered iv). Blood samples were obtained 60 min after LPS injection. Serum was separated from clotted blood samples by centrifugation (5 min, 5000*g*, room temperature) and analyzed for levels of TNF-α by ELISA assay (R&D Systems) according to the manufacturer's directions. Results are shown as the mean ± SD of *n* = 8 mice per treatment group. All procedures involving animals were reviewed and approved by the Institutional Animal Care and Use Committee.

**Acknowledgment.** We gratefully acknowledge Dr. Mark Witmer for his assistance in providing experimental data for this manuscript and Dr. Kyoung S. Kim for his helpful discussions.

## References

- (1) (a) Porter, A. C.; Felder, C. C. The Endocannabinoid Nervous System: Unique Opportunities for Therapeutic Intervention. *Pharmacol. Ther.* **2001**, *90*, 45–60. (b) Williamson, E. M.; Evans, F. J. Cannabinoids in Clinical Practice. *Drugs* **2000**, *60* (6), 1303–1314. (c) Hollister, L. E. Health Aspects of Cannabis. *Pharmacol. Rev.* **1986**, *38*, 1–20.
- (2) Matsuda, L. A.; Lolait, S. J.; Brownstein, M. J.; Young, A. C.; Bonner, T. I. Structure of a Cannabinoid Receptor and Functional Expression of the Cloned cDNA. *Nature* **1990**, *346*, 561–564.
- (3) Munro, S.; Thomas, K. L.; Abu-Shaar, M. Molecular Characterization of a Peripheral Receptor for Cannabinoids. *Nature* **1993**, *365*, 61–65.
- (4) For a comprehensive review, see the following. Pertwee, R. G. Pharmacology of Cannabinoid CB<sub>1</sub> and CB<sub>2</sub> Receptors. *Pharmacol. Ther.* **1997**, *74*, 129–180.
- (5) Wagner, J. A.; Varga, K.; Ellis, E. F.; Rzigalinski, B. A.; Martin, B. R.; Kunos, G. Activation of Peripheral Cannabinoid Receptors in Haemorrhagic Shock. *Nature* **1997**, *390*, 518–521.
- (6) (a) Germain, N.; Boichot, E.; Advenier, C.; Berdyshev, E. V.; Lagente, V. Effect of the Cannabinoid Receptor Ligand, WIN 55,212-2 on the Superoxide Anion and TNF- $\alpha$  Production by Human Mononuclear Cells. *Int. Immunopharmacol.* **2002**, *2*, 537–543. (b) Smith, S. R.; Terminelli, C.; Denhardt, G. Modulation of Cytokine Responses in *Corynebacterium Parvum*-Primed Endotoxemic Mice by Centrally Administered Cannabinoid Ligands. *Eur. J. Pharmacol.* **2001**, *425*, 73–83. (c) Smith, S. R.; Terminelli, C.; Denhardt, G. Effects of Cannabinoid Receptor Agonist and Antagonist Ligands on Production of Inflammatory Cytokines and Anti-inflammatory Interleukin-10 in Endotoxemic Mice. *J. Pharmacol. Exp. Ther.* **2000**, *293*, 136–150. (d) Jagger, S. I.; Sellaturay, S.; Rice, A. S. The Endogenous Cannabinoid Anandamide, but Not the CB<sub>2</sub> Ligand Palmitoylethanolamide, Prevents the Viscero-Visceral Hyper-Reflexia Associated with Inflammation of the Rat Urinary Bladder. *Neurosci. Lett.* **1998**, *253*, 123–126. (e) Richardson, J. D.; Kilo, S.; Hargreaves, K. M. Cannabinoids Reduce Hyperalgesia and Inflammation via Interaction with Peripheral CB<sub>1</sub> Receptors. *Pain* **1998**, *75*, 111–119. (f) Berdyshev, E.; Boichet, E.; Corbel, M.; Germain, N.; Lagente, V. Effects of Cannabinoid Receptor Ligands on LPS-Induced Pulmonary Inflammation in Mice. *Life Sci.* **1998**, *63*, 125–129.
- (7) For recent reviews, see the following. (a) Di Marzo, V.; De Petrocellis, L.; Bisogno, T. Endocannabinoids Part I: Molecular Basis of Endocannabinoid Formation, Action and Inactivation and Development of Selective Inhibitors. *Emerging Ther. Targets* **2001**, *5* (2), 241–265. (b) Pertwee, R. G. Cannabinoid Receptor Ligands: Clinical and Neuropharmacological Considerations, Relevant to Future Drug Discovery and Development. *Exp. Opin. Invest. Drugs* **2000**, *9* (7), 1553–1571.
- (8) D'Ambra, T. E.; Estep, K. G.; Bell, M. R.; Eissenstat, M. A.; Josef, K. A.; Ward, S. J.; Haycock, D. A.; Baizman, E. R.; Casiano, F. M.; Beglin, N. C.; Chippari, S. M.; Grego, J. D.; Kullnig, R. K.; Daley, G. T. Conformationally Restrained Analogs of Pravastatin: Nanomolar Potent, Enantioselective, (Aminoalkyl)indole Agonists of the Cannabinoid Receptor. *J. Med. Chem.* **1992**, *35*, 124–135.
- (9) Showalter, V. M.; Compton, D. R.; Martin, B. R.; Abood, M. E. Evaluation of Binding in a Transfected Cell Line Expressing a Peripheral Cannabinoid Receptor (CB<sub>2</sub>): Identification of Cannabinoid Receptor Subtype Selective Ligands. *J. Pharmacol. Exp. Ther.* **1996**, *278*, 989–999.
- (10) (a) Martin, B. R.; Compton, D. R.; Thomas, B. F.; Prescott, W. R.; Little, P. J.; Razdan, R. K.; Johnson, M. R.; Melvin, L. S.; Mechoulam, R.; Ward, S. J. Behavioral, Biochemical, and Molecular Modeling Evaluations of Cannabinoid Analogs. *Pharmacol. Biochem. Behav.* **1991**, *40*, 471–478. (b) Compton, D. R.; Gold, L. H.; Ward, S. J.; Balster, R. L.; Martin, B. R. Aminoalkylindole Analogs: Cannabinomimetic Activity of a Class of Compounds Structurally Distinct from  $\Delta^9$ -Tetrahydrocannabinol. *J. Pharmacol. Exp. Ther.* **1992**, *263*, 1118–1126.
- (11) Hynes, J., Jr.; Leftheris, K.; Wu, H.; Pandit, C.; Chen, P.; Norris, D. J.; Chen, B.-C.; Zhao, R.; Kiener, P. A.; Chen, X.; Turk, L. A.; Patil-Koota, V.; Gillooly, K. M.; Shuster, D. J.; McIntyre, K. W. C-3 Amido-Indole Cannabinoid Receptor Modulators. *Bioorg. Med. Chem. Lett.* **2002**, *12*, 2399–2402.
- (12) Eissenstat, M. A.; Bell, M. R.; D'Ambra, T. E.; Alexander, E. J.; Daum, S. J.; Ackerman, J. A.; Gruett, M. D.; Kumar, V.; Estep, K. G.; Olefirowicz, E. M.; Wetzel, J. R.; Alexander, M. D.; Weaver, J. D., III; Haycock, D. A.; Luttinger, D. A.; Casiano, F. M.; Chippari, S. M.; Kuster, J. E.; Stevenson, J. I.; Ward, S. E. Aminoalkylindoles: Structure–Activity Relationships of Novel Cannabinoid Mimetics. *J. Med. Chem.* **1995**, *38*, 3094–3105.
- (13) A similar syn conformation of structurally related WIN-55212-2 cannabinoid ligand has also been implicated as the bioactive conformation. Reggio, P. H.; Basu-Dutt, S.; Barnett-Norris, J.; Castro, M. T.; Hurst, D. P.; Seltzman, H. H.; Roche, M. J.; Gilliam, A. F.; Thomas, B. F.; Stevenson, L. A.; Pertwee, R. G.; Abood, M. E. The Bioactive Conformation of Aminoalkylindoles at the Cannabinoid CB<sub>1</sub> and CB<sub>2</sub> Receptors: Insights Gained from (*E*- and *Z*-Naphthylidene Indenes. *J. Med. Chem.* **1998**, *41*, 5177–5187.
- (14) Clark, R. D.; Muchowski, J. M.; Fisher, L. E.; Flippin, L. A.; Repke, D. B.; Souchet, M. Preparation of Indoles and Oxindoles from *N*-(*tert*-Butoxycarbonyl)-2-alkylanilines. *Synthesis* **1991**, *10*, 871–878.
- (15) Yoshida, T.; Matsuura, N.; Yamamoto, K.; Doi, M.; Shimada, K.; Morie, T.; Kato, S. Practical Synthesis of 1*H*-Indazole-3-carboxylic Acid and Its Derivatives. *Heterocycles* **1996**, *43*, 2710–2712.
- (16) Experimental conditions were modified from the following. Clark, R. D.; Miller, A. B.; Berger, J.; Repke, D. B.; Weinhardt, K. K.; Kowalczyk, B. A.; Eglen, R. M.; Bonhaus, D. W.; Lee, C.-H.; Michel, A. D.; Smith, W. L.; Wong, E. H. F. 2-(Quinuclidin-3-yl)pyrido[4,3-*b*]indol-1-ones and Isoquinolin-1-ones. Potent Conformationally Restricted 5-HT<sub>3</sub> Receptor Antagonists. *J. Med. Chem.* **1993**, *36*, 2645–2657.
- (17) Suchocki, J. A.; Everette, L. M.; Martin, T. J.; George, C.; Martin, B. R. Synthesis of 2-*exo*- and 2-*endo*-Mecamylamine Analogues. Structure–Activity Relationships for Nicotinic Antagonism in the Central Nervous System. *J. Med. Chem.* **1991**, *34*, 1003–1010.
- (18) Mohamadi, F.; Richards, N. G. J.; Guida, W. C.; Liskamp, R.; Lipton, M.; Cauffield, C.; Chang, G.; Hendrickson, T.; Still, W. C. MacroModel—An Integrated Software System for Modeling Organic and Bioorganic Molecules Using Molecular Mechanics. *J. Comput. Chem.* **1990**, *11*, 440.
- (19) Halgren, T. A. Merck Molecular Force Field. I. Basis, Form, Scope, Parameterization, and Performance of MMFF94. *J. Comput. Chem.* **1996**, *17*, 490.
- (20) Shenkin, P. S.; McDonald, D. Q. Cluster Analysis of Molecular Conformations. *J. Comput. Chem.* **1994**, *15*, 899.
- (21) *Jaguar*, version 4.0; Schrödinger, Inc.: Portland, OR, 1991–2000.

JM020329Q